Efficiency of the Galvanostatic Formation of Anodic Antimony Oxide in Oxalic Acid Solutions

Ch. Girginov*, E. Lilov, S. Kozhukharov and **V. Lilova**

University of Chemical Technology and Metallurgy,
8 Kl. Ohridski blvd., 1756 Sofia, Bulgaria

*Corresponding author: girginov@uctm.edu

Received 08/07/2019; accepted 25/06/2021
https://doi.org/10.4152/pea.2022400203

Abstract
The formation of thick anodic oxide films on antimony in diluted solutions of oxalic acid ($CO(OH)_2$) was studied under galvanostatic and isothermal conditions. The film formation was always accompanied by a dissolution process which strongly depended on the growth conditions. The formation efficiency, as determined by the dissolved metal amount, was affected by the $CO(OH)_2$ concentration, the current density and the anodization time. The dissolved antimony amount increased with higher $CO(OH)_2$ concentrations and anodization time, and with lower current densities. The analysis of the total current density suggests the occurrence of a formed film and a dissolving component. According to the calculations, the anodic oxides composition is close to Sb_2O_3. The growth of anodic Sb_2O_3 took place at high electric fields within the oxide film. The thicknesses of the formed films were calculated by taking into account their dissolution. The film formation efficiency was determined at various current densities.

Keywords: antimony anodic dissolution, film formation efficiency, galvanostatic anodization and electric field intensity.

Introduction

Metals anodic dissolution is an important topic for both practice (battery design, materials finishing, corrosion protection, metal digestion and others) [1-3] and theory [4, 5]. Anodic oxide films on antimony can be formed in different aqueous or non-aqueous electrolyte solutions. The use of various acidic solutions, such as sulfuric [6-11], phosphoric [12-15], oxalic [16-18] and hydrofluoric acids [19] has been reported. In all cases, appreciable oxide dissolution during the film formation has been ascertained. The oxide dissolution continues even without polarization in diluted aqueous solutions of H_2SO_4 [11] and $CO(OH)_2$ [16].

In order to explore the oxide films anodic formation under well-defined conditions, a galvanostatic and isothermal regime is frequently used, but the kinetics of anodic oxide growth on antimony has been found to strongly depend on the electrolyte forming conditions, nature and concentration. Besides the classical linear increase in the forming voltage (U_{form}) with time (t), passed charge density (Q_{total}), S-shaped curves, induction periods and maxima in the kinetic dependencies have been observed. Anodization in $CO(OH)_2$ diluted aqueous solutions was found to proceed up to high voltages, thus leading to the formation of relatively thick oxide films [16-18].

In $CO(OH)_2$ solutions, with concentrations in the range from 0.001 to 0.02 M, two-stage kinetic curves were observed [17]. They were linear only during the first anodization step, for charge densities up to 6 C cm^{-2}. During the second one, the increase in U_{form} slowed down, and electrical break down occurred.
In this work, antimony oxide films formation and dissolution during their anodic oxidation in $CO(OH)_2$ were studied, in order to estimate the electrolyte concentration, current density and process duration influence on the films formation efficiency (λ) and thickness (d).

Experimental

Electrode preparation

The working electrodes were prepared from high purity polycrystalline metallic antimony (99.999% Sb), from American Elements, with a working area of 2.5 cm^2. The surface was isolated with a thick layer of epoxy resin. The electrodes were mechanically polished with a P 4000 sand paper (5 μm), and were then washed with neutral detergent and double distilled water.

Conditions for film formation

Anodization was carried out at constant total current density ($J_{total} = 0.8 - 20\,mA\,cm^{-2}$), at 20 ºC. A two-electrode cell with a golden plate as counter-electrode was used, connected to a high voltage galvanostat (600 V, 0.5 A). The electrolytes were intentionally not stirred, in order to avoid the influence of hydrodynamic effects. Various $CO(OH)_2$ aqueous solutions, with concentrations from 0.001 to 0.02 M, were used as forming electrolytes. The film formation was carried out only during the first anodization stage, thus corresponding to the $U_{form}(t)$-curves linear part. In all experiments, the passed charge density did not exceed 0.6 C cm^{-2}. The final forming voltage was in the range from 100 to 150 V.

Used equipment

Kinetic curves showing U_{form} dependence on t were registered by a precision multimeter (Mastech MS 8050) and a PC-based data acquisition system. The dissolved Sb amount during anodization was determined by the Inductively Coupled Plasma Optical Emission Spectrometry (ICP-OES) method. Further, an interferometric method was used to estimate the formed oxide films thicknesses.

Results and discussion

Influence of the anodizing parameters on the dissolved antimony amount

The influence of $CO(OH)_2$ concentration (C), total current density (J_{total}) and anodizing time (t) on the dissolved Sb amount was studied. These data were further used for calculating the film formation efficiency.

$CO(OH)_2$ *concentration influence*

The $CO(OH)_2$ concentration influence on the dissolved Sb amount was determined by ICP-OES, for specimens anodized at current densities from 2 to 10 mA cm^{-2}, in $CO(OH)_2$ aqueous solutions with concentrations from 0.001 to 0.02 M (Fig. 1).

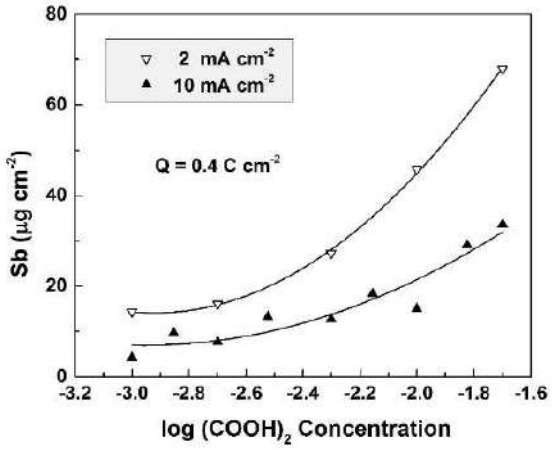

Figure 1. Dissolved Sb amount as a function of the electrolyte concentration for Sb oxide films formed in $CO(OH)_2$ solutions, at two current densities.

In all experiments, the total passed charge density was 0.4 C.cm^{-2}. This value, as well as the concentration range, was chosen to keep the film growth in the kinetic curve linear part.
As seen in the figure, for both current densities, the dissolved Sb amount increased with higher $CO(OH)_2$ concentrations, which was an expected result. On the other hand, larger amounts of dissolved Sb were obtained at lower current densities. For one and the same passed charge density, lower current densities would correspond to longer anodization times and film exposure to the more or less aggressive solution. Hence, it is expected that the chemical dissolution should play a role in the film dissolution process.

Current density influence
Applied J_{total} influence was studied in two electrolytes with concentrations of 0.001 and 0.01 M, in the range from 0.8 to 20 mA cm^{-2}. In all experiments, a constant value of 0.4 C cm^{-2} was chosen for the charge density. The dissolved Sb amount in both electrolytes depended on the anodization current density (Fig. 2).

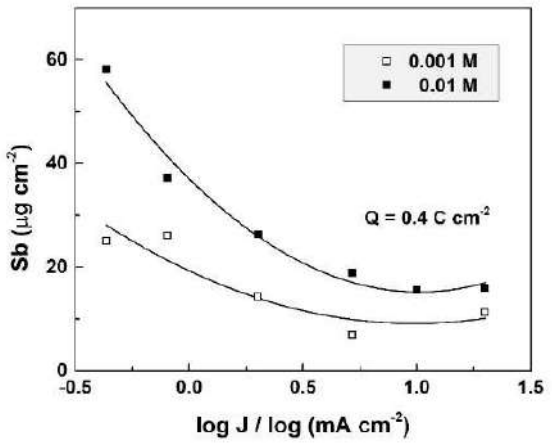

Figure 2. Dissolved Sb amount in 0.01 M and 0.001 M $CO(OH)_2$, as a function of the current density.

The results logically point to increasing amounts of dissolved Sb with higher electrolyte concentrations and lower current density, as it was found for other metals [20].

Anodization time influence

The influence of anodization time (t) or of the passed charge density (Q_{total}) on the dissolved Sb amount was studied in 0.01 M $CO(OH)_2$, at four current densities. The results are presented in Fig. 3. They confirmed once more that the decrease in current density leads to an increase in the dissolved Sb amount. A quite surprising feature of the shown dependences is their linearity, as observed for all used current densities.

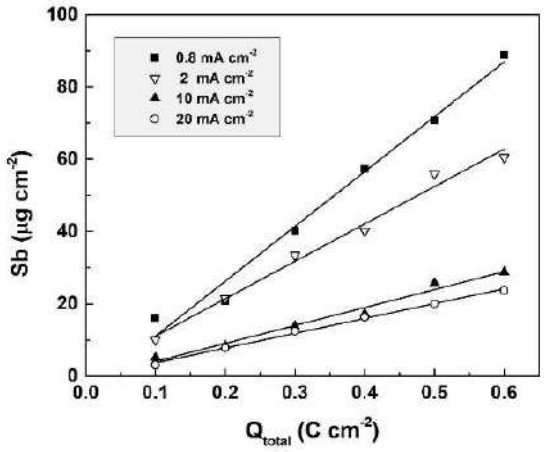

Figure 3. Dissolved Sb amount during anodization in 0.01 M $CO(OH)_2$, at different current densities.

So to assess the impact of chemical dissolution during anodic polarization, experimental exposure of formed films, with 0.8 mA cm-2, to 0.01 M CO(OH)2, was performed over 750 secs (Q_{total} = 0.6 C cm^{-2}). After this, the dissolved Sb amounts were measured (approx. 1 μg cm^{-2}). This amount was around 1.1% of the overall dissolved Sb during anodic polarization. Thus, chemical dissolution during anodic polarization could be neglected. A proportional correlation of the dissolved Sb amount with Q_{total} (t) was observed. The dissolution current density values (J_{diss}) during anodic polarization can be estimated by the charge passed for Sb electrochemical dissolution (Q_{diss}). This enables the calculation of the film formation efficiency.

Calculation of the film dissolution charge density

Using the data obtained from the ICP-OES method, the Q_{diss} charge apparently spent for the chemical and electrochemical Sb dissolution was calculated by the following expression:

$$Q_{diss} = \frac{m_{Sb} z F}{M_{Sb}} \qquad (1)$$

where m_{Sb} is the dissolved Sb mass, M_{Sb} is Sb atomic mass (M_{Sb} = 121.76 g/mol^{-1}), z is the number of exchanged charges, while Sb dissolves to Sb^{3+}, z = 3, and F is Faraday constant (96485 C mol^{-1}).

In Fig. 4, Q_{diss} is presented as a function of the total charge passed (Q_{total}) during anodization, in 0.01 M $CO(OH)_2$, at different current densities, in the range from 0.8 to 20 mA.cm^{-2}. Proportionality was ascertained between Q_{diss} and Q_{total}, thus justifying once more the approach chosen. As shown in the figure, the charge spent for dissolution increases with lower current densities.

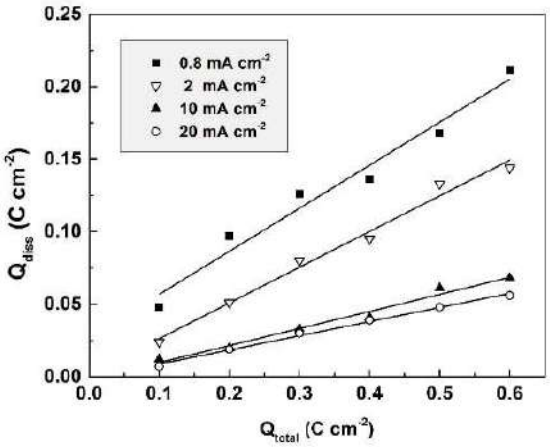

Figure 4. Dependence of the apparent charge spent for Sb dissolution on the total charge passed during anodization, in 0.01 M $CO(OH)_2$, at various current densities.

The knowledge of Q_{diss} and Q_{total} allows the calculation of the charge spent for the film formation (Q_{form}), as the difference of Q_{total} - Q_{diss}, at a given current density.

Sb oxide films thickness determination

One of the important characteristics of anodic oxide films is their thickness (d). The theoretical film thickness can be calculated from Faraday's law, by introducing the total passed charge density:

$$Q_{total}=J_{total}t \qquad (2)$$

In this case, it has to be assumed that the total current is entirely ionic, and that no electrochemical dissolution or electronic conduction occurs, so that $J_{total} = J_{ionic}$. The film thickness is then calculated:

$$d = \frac{M_{oxide}Q_{total}}{zF\rho_{oxide}} \qquad (3)$$

where M_{oxide} is the Sb oxide molecular mass and ρ_{oxide} is its density, z is the number of exchanged electrons and F is the Faraday constant. Problems related with the Sb oxide films stoichiometry have arisen a long time ago.

Different opinions have been expressed, suggesting Sb_2O_3, Sb_2O_5, Sb_2O_4 [19], or even more complex compositions. In most studies, however, the Sb_2O_3 composition has been upheld [14, 15].

Assuming two compositions of the obtained films (Sb_2O_3 and Sb_2O_5), their thicknesses were calculated in parallel using equation (3). The calculated values were then compared to those experimentally determined by standard interferometric methods.

The calculations have shown that only the acceptance of Sb_2O_3 (M_{Sb2O3} = 291.5 g.mol^{-1}, ρ_{Sb2O3} = 5.2 g.cm^{-3} and z = 6) would result in thicknesses comparable to those determined by the optical method.
The experimental thicknesses (d) of oxide films formed during anodization in 0.01 M CO(OH)2, at three current densities, are presented in Fig. 5, in juxtaposition with the calculated theoretical films thicknesses.

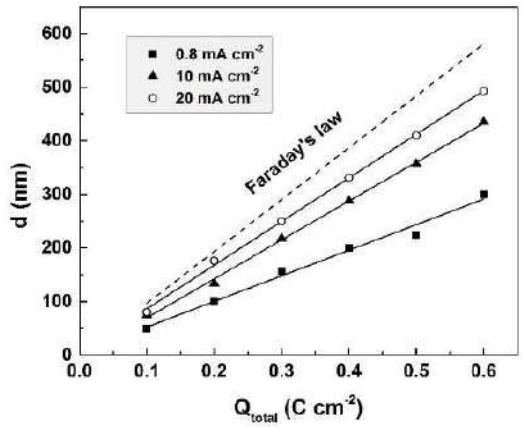

Figure 5. Experimental thicknesses of oxide films formed during anodization at three current densities. Calculated theoretical thicknesses are plotted for comparison.

In all cases, experimental thicknesses are lower than theoretical ones. Anodization at higher current densities results in thicker Sb_2O_3-films. These results are in full agreement with the established reduction of the dissolved Sb amount with higher current densities. The charge spent in film formation, $Q_{form} = Q_{total} - Q_{diss}$, was calculated and plotted versus the total passed charge (Fig. 6).

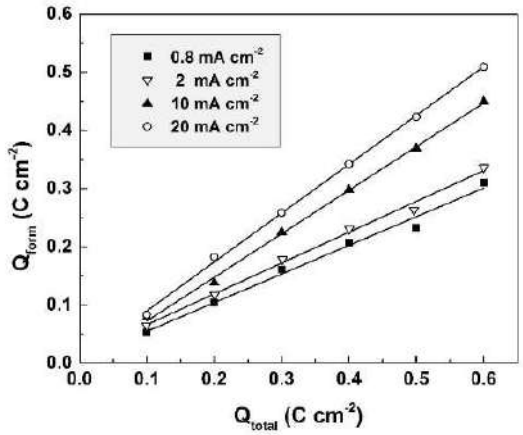

Figure 6. Dependence of the charge density passed for the antimony oxide film formation on the total charge passed during anodization.

Q_{form} found values allowed to correct the calculated film thicknesses from equation (3) for film dissolution, taking again Sb_2O_3 as the oxide composition. The film thickness corrected values were compared with the experimental ones (Fig. 7).

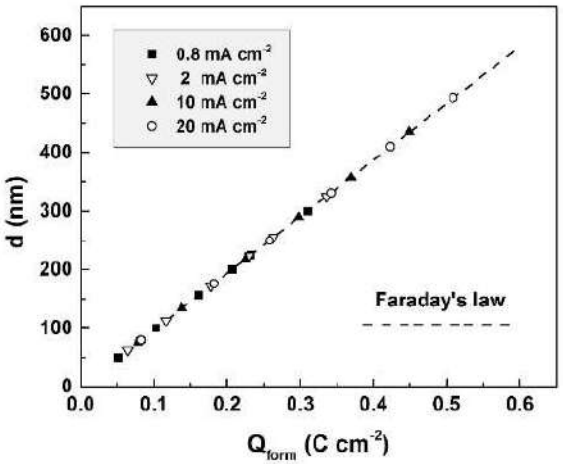

Figure 7. Anodic Sb_2O_3-films thicknesses, corrected for dissolution, in dependence of the charge passed for their formation (broken line). Symbols denote optically measured experimental thicknesses.

The excellent agreement between the corrected and experimental thickness values indicates, on one hand, the reliability of the used optical method, and on the other, the absence of measurable electronic conductivity during the film formation.

Electric field intensity calculation

The electric field (E) intensity (or the so-called field strength) during anodization is calculated from the following expression:

$$E = \frac{U_{form}}{d} \qquad (4)$$

The Sb isothermal and galvanostatic anodization, in various electrolytes, leads to the formation of films with different dielectric properties. E values in 1 M H_3PO_4 reached up to 6.5×10^5 V cm^{-1} [13], and in buffered phosphate electrolytes reached 2.25×10^6 V cm^{-1} [15]. The latter value is usually related to the presence of high electric fields within the oxide film, and the current is assumed to be prevailingly ionic. It was of interest to determine E value during Sb anodic polarization in 0.01 M $CO(OH)_2$. Under the used conditions, a E value = 2.37×10^6 V cm^{-1} was calculated, thus indicating a high-field film formation in the whole current density range, studied alongside with a negligible electronic component of the current.

Film formation efficiency

Anodic film formation efficiency (λ) calculations appeared to be an easy task. Q_{form}- values ratios and the corresponding Q_{total} values were calculated for four different current densities to furnish λ values, according to the expression:

$$\lambda = 100\,\frac{Q_{form}}{Q_{total}} \qquad (5)$$

The film formation efficiency is plotted in Fig. 8 against the total charge passed during Sb anodization in 0.01 M $CO(OH)_2$.

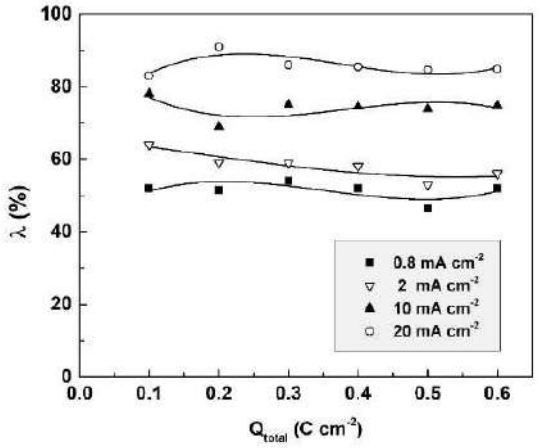

Figure 8. Sb_2O_3-film formation efficiency in 0.01 M $CO(OH)_2$, at four current densities, in dependence of the total passed charge density.

As seen in the figure, the anodic film formation efficiency proved to remain practically constant during the anodization, at a given current density, and to increase with higher J. The λ constancy implies a constant film dissolution rate; the latter might explain the proportionality between total charge density and total dissolved Sb amount.

Conclusions

Sb anodic oxidation in diluted $CO(OH)_2$ solutions led to the formation of relatively thick oxide films, but which always suffered dissolution. The dissolution process was strongly affected by $CO(OH)_2$ concentration, current density conditions and anodization time. The dissolved Sb amount increased with longer times and total passed charge density, and decreased with higher current densities. The linear dependence between the dissolved Sb amount and the total charge permitted the calculation of an apparent charge spent for dissolution, as well as of the charge spent for films formation. Using these data, the anodic oxide composition was determined as being Sb_2O_3. The calculated films thicknesses proved to be in excellent agreement with the experimental values determined by a standard interferometric method, and finally, the film formation efficiency could be evaluated under different current density conditions. The efficiency was found not to depend on total charge density; it increased with higher current densities.

Acknowledgements

The authors wish to thank the National program "Young scientists and postdoctoral students", of the Ministry of Education and Science of the Republic of Bulgaria, for the financial support.

Authors' contributions

Ch. Girginov: conceived and designed the analysis; contributed with data or analysis tools; performed the analysis; wrote the paper. **E. Lilov**: conceived and designed the analysis; collected the data; wrote the paper. **S. Kozhukharov**: conceived and designed the analysis; contributed with data or analysis tools;

performed the analysis. **V. Lilova**: conceived and designed the analysis; contributed with data or analysis tools; performed the analysis.

References

1. Abbott AP, Frisch G, Hartley J, et al. Anodic dissolution of metals in ionic liquids. Prog Nat Sci: Mater Int. 2015;25:595-602. Doi: https://doi.org/10.1016/j.pnsc.2015.11.005
2. Lee H-J, Park In-J, Choi S-R, et al. Effect of Chloride on Anodic Dissolution of Aluminum in 4 M NaOH Solution for Aluminum-Air Battery. J Electrochem Soc 2017;164(4):A549-A554. Doi: https://doi.org/10.1149/2.0011704jes
3. Ogorodnikova VA, Kuznetsov Yu I, Chirkunov AA, et al. Inhibition of anodic dissolution of Mg90 alloy by adsorption layers of higher carboxylic acids. Int J Corros Scale Inhib. 2018;7(2):260-270. Doi: https://doi.org/10.17675/2305-6894-2018-7-2-11
4. Madrigal-Cano M, Hernández-Maya L, Manuel Hallen L, et al. Model for the Correlation between Anodic Dissolution Resistance and Crystallographic Texture in Pipeline Steels. Materials. 2018;11(8):1432. Doi: https://doi.org/10.3390/ma11081432
5. Vanaei HR, Eslami A, Egbewande A. A review on pipeline corrosion, in-line inspection (ILI), and corrosion growth rate models. Int J Pres Ves Pip. 2017;149: 43-54. Doi: https://doi.org/10.1016/j.ijpvp.2016.11.007
6. Metikoš-Huković M, Lovreček B. Electrochemical behaviour of the oxide covered antimony. Electrochim Acta. 1980;25(5):717-723. Doi: https://doi.org/10.1016/0013-4686(80)87084-8
7. Pavlov D, Bojinov M, Laitinen T, et al. Electrochemical behaviour of the antimony electrode in sulphuric acid solutions. Corrosion processes and anodic dissolution of antimony. Electrochim Acta. 1991;36(14):2087-2092. Doi: https://doi.org/10.1016/0013-4686(91)85213-Q
8. Bojinov M, Kanazirski I, Girginov A. A model for surface charge-assisted barrier film growth on metals in acidic solutions based on ac impedance measurements. Electrochim Acta. 1996;41(17):2695-2705. Doi: https://doi.org/10.1016/0013-4686(96)00124-7
9. Metikoš-Huković M, Babić R, Brinić S. EIS-in situ characterization of anodic films on antimony and lead–antimony alloys. J Power Sources. 2006;157(1):563-570. Doi: https://doi.org/10.1016/j.jpowsour.2005.07.079
10. Mogoda AS. Electrochemical behaviour of anodic oxide film on antimony in sulfuric acid solutions containing dichromate ions. Thin Solid Films. 2001;394(1-2):173-178. Doi:https://doi.org/10.1016/S0040-6090(01)01130-0
11. Mogoda AS, Abd El-Haleem TM. Anodic oxide film formation on antimony and its currentless dissolution in sulphuric acid containing some monocarboxylic acids. Thin Solid Films. 2003;441(1-2):6-12. Doi: https://doi.org/10.1016/S0040-6090(03)00876-9
12. Hefny MM, Badawy WA, Mogoda AS, et al. Electrochemical behaviour of anodic oxide films on antimony in phosphate solutions. Electrochim Acta. 1985;30(8):1017-1020. Doi: https://doi.org/10.1016/0013-4686(85)80166-3

13. Bojinov M, Kanazirski I, Girginov A. Anodic film growth on antimony in H_3PO_4 solutions. Electrochim Acta. 1995;40(7):873-878. Doi: https://doi.org/10.1016/0013-4686(94)00344-Z
14. Linarez Pérez OE, Pérez MA, López Teijelo M. Characterization of the anodic growth and dissolution of antimony oxide films. J Electroanal Chem. 2009;632(1-2):64-71. Doi: https://doi.org/10.1016/j.jelechem.2009.03.018
15. Linarez Pérez OE, Sánchez MD, López Teijelo M. Characterization of growth of anodic antimony oxide films by ellipsometry and XPS. J Electroanal Chem. 2010;645(2):143-148. Doi: https://doi.org/10.1016/j.jelechem.2010.04.023
16. Angelov IG, Girginov Ch, Klein E. Growth and dissolution of anodic antimony oxide in oxalic acid electrolytes. Bulg Chem Comm. 2011;43(1):144-149.
17. Lilov E, Girginov Ch, Klein E. Dissolution of antimony during its galvanostatic anodization in oxalic acid. Adv Nat Sci: Theory Appl. 2012;1:115-120.
18. Lilov E, Girginov Ch, Klein E. Anodic oxide films on antimony formed in oxalic acid solutions. Bulg. Chem. Comm. 2013;45(Special Issue A): 94-98.
19. El Wakkad SES, Hickling A. The Anodic Behavior of Antimony. J Phys Chem. 1953;57(2):203-206. Doi: https://doi.org/10.1021/j150503a015
20. Abbasa Q, Binder L. Anodic Dissolution of Refractory Metals in Choline Chloride Based Binary Mixtures. ECS Trans. 2011;33(30):57-67. Doi: https://doi.org/10.1149/1.3566089